Korean J. Chem. Eng., 34(2), 413-424 (2017)
DOI: 10.1007/s11814-016-0268-2

pISSN: 0256-1115
eISSN: 1975-7220

Adsorptive separation of CO_2 and CH_4 by the broom sorghum based activated carbon functionalized by diethanolamine

Elaheh Mehrvarz, Ali Asghar Ghoreyshi†, and Mohsen Jahanshahi

Chemical Engineering Department, Babol University of Technology, Shariati Street, Babol, Iran
(*Received 31 March 2016 • accepted 25 September 2016*)

Abstract−A low-cost activated carbon (AC) was produced from the broom sorghum stalk using KOH as the chemical activating agent, and then the surface of AC was functionalized with diethanolamine to enhance CO_2/CH_4 selectivity. Characteristics of pristine and DEA-functionalized ACs were determined through different analyses such as Boehm's method, BET, FT-IR, SEM, and TGA. The adsorption behavior of pure carbon dioxide and pure methane on these adsorbents was investigated in a temperature range of 288-308 K and pressure range of 0-25 bar using an apparatus based on a volumetric method. Results indicated that amine functionalization significantly improved the selectivity of CO_2/CH_4. The enhancement of CO_2 ideal adsorption selectivity over CH_4 from 1.51 for the pristine AC to 5.75 for the AC-DEA was attributed to adsorbate-adsorbent chemical interaction. The present DEA-functionalized AC adsorbent can be a good candidate for applications in natural gas and landfill gas purifications.

Keywords: Activated Carbon, Broom Sorghum, Carbon Dioxide, Methane, Functionalization, Diethanolamine

INTRODUCTION

There has been a significant increase in the production of natural gas as an efficient and clean fuel supply due to stringent environmental regulations [1-3]. Natural gas, which is rich in methane, typically 80 to 95%, is a promising source of global energy for the foreseeable future [4]. However, carbon dioxide (CO_2) is often found as a major impurity in raw natural gas extracted from many reservoirs. Carbon dioxide is an acidic and corrosive gas that causes some problems in natural gas storage and transportation, and its presence can reduce the energy content of natural gas [5,6]. Apart from these negative effects, on the basis of methane conversion to valuable products, enhancement in CH_4 purity is necessary for any improvement in process efficiency [7].

The consumption of natural gas is expected to grow by 50% over the next 20 years and the energy shortage situation is becoming more and more serious. As a result, methane from landfill gas is a rapidly growing source of natural gas [8]. Landfill gas is a by-product of the anaerobic decomposition of the biodegradable constituents of the landfill waste which are mainly composed of methane and carbon dioxide, with a mole percent of methane ranging from 45 to 65 [9]. Furthermore, natural gas as an energy resource has become the center of interest since it solves both the energy crisis and environmental pollution. Removal of CO_2 from CH_4 is a requisite step for purification of CH_4 from the landfill gas emissions [10]. There are several methods for CO_2 separation, including physical-chemical absorption, pressure swing adsorption (PSA), membrane separation and cryogenic distillation [4,11]. The most widely used technology for removal of CO_2 from CO_2/CH_4 gas mixtures is amine scrubbing. However, some drawbacks are associated with using liquid amine solutions for CO_2 separation. High energy consumption, equipment corrosion, solvent degradation in the presence of oxygen and loss of amine during regeneration are reasons which make it vital to look for other alternative processes [12].

Pressure swing adsorption technology has gained much attention in comparison to other techniques, particularly for CO_2 removal due to its low energy requirement, easy operation and low capital investment costs [8,13,14]. Therefore various porous materials such as activated carbons [15], zeolites [16], carbon molecular sieves [7] and metal-organic frameworks [17] have been investigated as sorbents in order to separate gas mixtures of CO_2 and CH_4. The most important aspect of the adsorption process is to develop a low cost adsorbent with a high adsorption capacity and selectivity. Activated carbons (ACs) occupy a prominent position among current adsorbents as a favorable option for use in gas purification. High surface area, large pore volume, favorable pore size distribution, the degree of polarity, lesser sensitivity to moisture and the possibility of easy recovery are the advantages of ACs that render them as efficient adsorbents for separation processes [18,19]. AC is mainly produced by thermal decomposition associated with physical/chemical activation of a wide range of different carbon containing source materials. Recently, low-cost and available lignocellulosic biomass residues such as cotton stalk, rice husk, corn cobs and fruit stone have proven to be potential precursors for synthesizing AC [20-23]. Broom sorghum stalk, one of these low cost agricultural wastes which has a reasonably high content of carbon, can be also utilized as raw material for AC preparation.

Although AC adsorbents show relatively high CO_2 adsorption capacity, the selectivity of these materials in the presence of other gases is poor [24]. To prevent this negative phenomenon, surface modification of ACs by a variety of methods has been greatly paid attention in recent years [25,26]. A further development of ACs is

†To whom correspondence should be addressed.
E-mail: aa_ghoreyshi@nit.ac.ir, aa_ghoreyshi@yahoo.com

either to control the pore size distribution (modification of pore size) or to modify its surface chemistry [22]. Due to acidic nature of CO_2, it has been recognized that increasing the alkalinity of ACs can strongly affect their selectivity. Therefore, promoting basic species such as amine groups on the surface of ACs is expected to be desirable for their application in the case of CO_2/CH_4 separation [27]. Alkanolamines are well-known amines with industrial importance for the removal of acidic gas components from several types of gas mixtures. Generally, they can be divided into three major groups: primary amine such as monoethanolamine, secondary amine such as diethanolamine, and tertiary amine such as triethanolamine. Distribution of alkanolamines on the surface of ACs enhances the benefits of the absorption process. An added advantage is that solids are easy to handle and do not give rise to corrosion problems caused by the circulation of very basic solutions [28, 29]. Surface functionalization of ACs with several types of amine functional groups and its application for CO_2 capture has been recently reported by other authors [13,30-32]. However, there are relatively few studies on the applications of these materials in CO_2 separation. To the best of our knowledge, there is no report on the preparation of amine modified broom sorghum based-AC for CO_2/CH_4 adsorptive separation. As a part of our continuing effort in adsorptive separation of CO_2/CH_4 [33], the main scope of the present work is the preparation of a cheap CO_2-philic adsorbent by amine functionalization of the AC synthetized from broom stalk. In this research, AC was prepared from the broom sorghum stalk by chemical activation with KOH and then functionalized with diethanolamine. The different properties of pristine AC and DEA-functionalized AC were characterized through Boehm's method, BET, SEM, FT-IR and TGA analyses. The equilibrium adsorption capacity for CO_2 and CH_4 on unmodified and modified samples was determined as a function of pressure at different temperatures and then analyzed in terms of suitable model isotherms. The adsorption kinetics and thermodynamics were also evaluated to assess the effectiveness and thermal behavior of adsorption process.

MATERIALS AND METHODS

1. Materials

Broom sorghum stalks were used as a cheap and locally available raw material for AC preparation. The precursor was collected from broom farms of Amirkola in the northern region of Iran. Hydrochloric acid 37% (HCl), potassium hydroxide 85% (KOH), anhydrous ethanol 99% (CH_2O_5) and Nitric acid 65% (HNO_3) were obtained from Merck Company. Diethanolamine (DEA) was purchased from Daejung Company. Carbon dioxide, methane, nitrogen and helium gases with a purity of 99.99% were supplied by Technical Gas Services, UAE.

2. Preparation of AC

Broom stalks were properly washed with distilled water and then dried in an oven at 383 K for 24 h. The dried stalks were crushed and sieved in the range of 0.3-0.6 mm. The carbonization system used to prepare the carbonaceous material consisted of a stainless steel vertical reactor surrounded by an electrical furnace. The as-sieved particles were carbonized under N_2 atmosphere at 623 K for 30 min to make a char easily mixable with activating solution. After cooling in a nitrogen flow, the obtained char was impregnated in a solution of potassium hydroxide (KOH) with the impregnation mass ratio of 1.5 (mass of dried stalks to agent). The liquid/solid mixture was stirred continuously for 6 h at 358 K. This mixture was then oven-dried at 383 K for 48 h. Impregnated precursor was placed in the pre-described carbonization furnace and pyrolyzed at 1,073 K, holding time of 1 h and heating rate of 10 K min^{-1} under a nitrogen flow rate of 150 mL min^{-1} STP. Following the activation process, the sample was cooled to room temperature under the same nitrogen flow and then removed from the reactor. The product was washed with 0.05 M HCl solution under agitation for 1 h to remove the activating agent from the material. The AC was separated from the solution by filtration and rinsed several times with hot and cold distilled water, respectively, until a neutral pH was achieved in the filtrate. Finally, the prepared AC was dried overnight at 383 K and placed in a desiccator.

3. Chemical Functionalization of AC

Grafting amine containing compound on the surface of prepared AC was performed using a two-stage modification. At the first stage, 1 g of pristine AC was added to 100 ml of nitric acid 5 M in order to increase the amount of oxygen surface groups. The solution was refluxed under magnetic stirring equipped with reflux condenser, thermometer and oil bath for proper heat distribution at 363 K for 3 h. After cooling the solution to room temperature, the sample was washed several times with distilled water after filtration until its pH increased to neutral value. The oxidized AC was then dried in an oven at 353 K for 8h. At the second stage of modification, 1 g of oxidized AC was added to 50 mL of diethanolamine solution. After that the mixture was refluxed at 343 K under stirring for 72 h, the final product was filtered, washed with ethanol to remove excess amine and then oven-dried at 353 K for 8 h. The amine functionalized AC was represented as AC-DEA.

4. Characterization

The chemical composition of broom sorghum stalk and prepared ACs was determined using CHNS elemental analyzer. The moisture, volatile matter and ash content of the broom stalk and prepared AC were characterized by standard test procedures according to ASTM D2867, ASTM D5832-98 and ASTM D2866-94, respectively. The morphology of both ACs including pristine AC and AC-DEA was analyzed by scanning electron microscopy (SEM) at an accelerating voltage of 15 kV. The surface chemistry of the adsorbents was evaluated by FTIR spectrometer using KBr pellet technique in the frequency range of 400-4,000 cm^{-1}. The N_2 adsorption/desorption isotherms were measured at 77 K using an adsorption apparatus (BELSORP, BEL Japan Inc.) to determine textural characteristics of the samples. The specific surface area was determined by the Brunauer-Emmett-Teller (BET) method. Total pore volume was calculated based on the liquid nitrogen adsorbed volume at the relative pressure of 0.99, and the micropore volume was obtained according to the t-plot method. The mesopore and micropore size distribution were determined by applying the Barrett-Joyner-Halenda (BJH) and micropore (MP) method, respectively. Thermogravimetric analysis (TGA) was carried out under nitrogen atmosphere at the heating rate of 25 °C min^{-1}, between 25 and 800 °C to study the thermal stability of the adsorbents. Boehm titration [34], the acid-base titration method, was used to determine

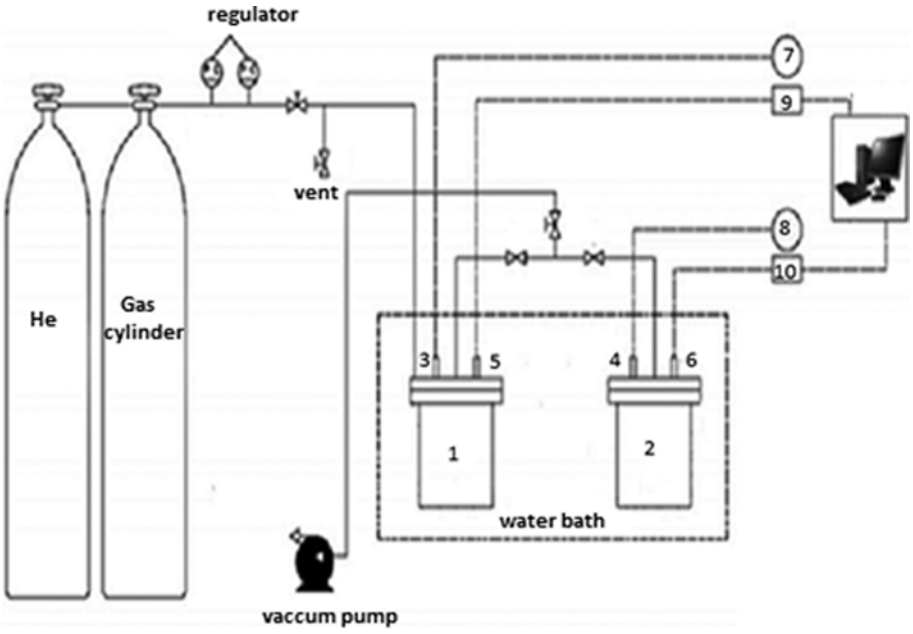

Fig. 1. Schematic diagram of the volumetric adsorption apparatus.

1. Pressure cell
2. Adsorption cell
3, 4. Temperature probe
5, 6. Pressure transducer
7, 8. Temperature digital indicator
9, 10. Pressure digital indicator

the concentration of different functional groups present on adsorbents' surfaces. A 0.2 g mass of each sample (unmodified and amine modified) was placed in a 50-ml Erlenmeyer flask containing 25 ml of 0.025 N NaOH, 0.025 N Na_2CO_3, 0.025 N $NaHCO_3$ and 0.025 N HCl. The flasks were sealed and agitated at 120 rpm for 24 h at temperature of 298 K and then filtered; 10 ml of the filtrate was pipetted and titrated with HCl (0.025 N) or NaOH (0.025 N) solutions. The numbers of acidic sites were determined under the assumption that NaOH (0.025 N) neutralizes carboxylic, lactonic, and phenolic groups, and Na_2CO_3 neutralizes carboxylic and lactonic groups, and $NaHCO_3$ neutralizes only carboxylic groups. The numbers of total basic sites were measured from the amount of used HCl (0.025 N).

5. Gas Adsorption Measurement

The volumetric adsorption set up used for the amount of gas adsorption on the AC, before and after amine functionalization, was similar to that used in our previous works [35-38]. Fig. 1 shows a schematic representation of the experimental set-up. Basically, it consisted of two high-pressure stainless steel cells called as pressure and sample cells, a set of valves and a couple of high pressure transducers with the maximum pressure 60 bar connected to the computer to record the changes in pressure during various stages of adsorption. Both cells were put in a water bath to keep the temperature constant during the gas adsorption. Prior to the adsorption study, adsorbents were degassed at 393 K for about 24 h and the system was evacuated by vacuum pump. In addition, the He gas was used as non-adsorbing gas to determine the dead volume. The gas adsorption experiments were performed using high purity CO_2 (99.99%) and methane (99.99%) at pressures ranging from 0 to 25 bar at different temperatures (288, 298 and 308 K). The choices of temperature and pressure ranges were based on the actual industrial consideration. Because CH_4/CO_2 separation by an adsorption column, typically a PSA unit, needs adsorption at high pressure (5-25 bars) and desorption at reduced low pressures. However, a precooling system is needed to lower the flue gas temperature for an effective separation. The amount of gas adsorbed on prepared adsorbents was calculated by the SRK equation of state in MATLAB program.

6. Adsorption Isotherms

Equilibrium data are of the most important parameters which provide the basis for the design of an adsorption system. There are many well-established isotherm models for predicting the equilibrium adsorption data in a wide range of pressure at a constant temperature. In this study, the gas adsorption data were fitted by means of three common and practical adsorption isotherms models, Langmuir [39], Freundlich [40] and Langmuir-Freundlich (Sips) [5], which are widely used for modeling of gas-separation processes. The models' equations with their parameters are shown in Table 1.

7. Equilibrium Selectivity

Equilibrium selectivity is a predominant scientific basis for adsorbent selection, and diffusion rate is generally secondary in importance. Equilibrium selectivity of the adsorbent as a measure of its ability in adsorption process at the pressure and temperature range of operation is defined by the following equation:

Table 1. Isotherm equations with their parameters

Model	Equation	Parameters
Langmuir	$q = q_m \frac{K_L P}{1 + K_L P}$	q_m (mmol g^{-1}), K_L (bar^{-1})
Freundlich	$q = K_F P^{1/n}$	K_F (mmol g^{-1} $bar^{-1/n}$), n (-)
Sips	$q = q_m \frac{(K_S P)^{1/n}}{1 + (K_S P)^{1/n}}$	q_m (mmol g^{-1}), Ks (bar^{-1}), n (-)

Table 2. Ultimate and proximate analysis of the raw material and pristine AC

Sample	Ultimate analysis					Proximate analysis			
	Carbon	Hydrogen	Nitrogen	Sulfur	Oxygen[a]	Moisture	Volatile mater	Ash	Fixed carbon[a]
Broom stalk	46.47	5.69	1.09	0	46.75	6.63	81.81	1.09	10.47
Pristine AC	74.01	4.71	1.87	0	19.41	4.29	30.8	2.71	62.2

[a]Calculated by difference

$$S_{AB}=\frac{x_A/y_A}{x_B/y_B} \quad (1)$$

where component A is the stronger adsorbate and B is the weaker adsorbate. X_A and X_B are the molar fractions of components A and B in the adsorbed phase, Y_A and Y_B are the molar fractions of components A and B in the gas phase. If the isotherms are linear or pressure is small enough to keep the isotherms in the linear range, ideally, the selectivity is described by the ratio of the adsorbed amount of pure components [41]:

$$S=\frac{n_A}{n_B} \quad (2)$$

8. Adsorption Kinetics

Adsorption kinetics is an important factor for evaluating adsorption performance of a sorbent. A wide variety of kinetic models have been proposed to quantitatively describe the adsorption process and to identify the adsorption mechanism. In this study, for modeling the adsorption kinetics, three types of models were used: pseudo-first-order, pseudo-second-order and pseudo-nth-order [38,42]. It is thought that instead of assuming the order of the reaction as 1 or 2, the direct calculation of the order of the adsorption reaction is a more appropriate method. Thus, nth-order kinetic model was utilized. The fractional order of this model describes the complexity of the reaction mechanisms and therefore can be an evidence for the occurrence of more than one reaction pathway.

Above mentioned kinetic models are given by the following equations:

$$q_t=q_e(1-e^{-k_1 t}) \quad \text{Pseudo-first-order}$$

$$q_t=\frac{k_2 q_e^2}{1+k_2 q_e t} \quad \text{Pseudo-second-order}$$

$$q_t=q_e-[(q_e)^{1-n}+(n-1)k_n t]^{1/1-n} \quad \text{Pseudo-nth-order kinetic}$$

where K_1 (s^{-1}), K_2 (g $mmol^{-1}$ s^{-1}) and K_n (s^{-1}) are rate constants, n is the order of kinetic equation, q_t (mmol g^{-1}) and q_e (mmol g^{-1}) represent the adsorption capacities of the sorbent at a specific time (s) and equilibrium time (s), respectively.

9. Adsorption Thermodynamic

One of the basic quantities in adsorption studies is the isosteric heat, which reflects the enthalpy change before and after the adsorption process. The isosteric heat of adsorption is a measure of the strength of interaction between gas molecules and the surface of adsorbent. The isosteric heat for gas adsorption can be determined as a function of surface loading by obtaining the slopes of the plots of lnP versus 1/T at a constant amount of adsorbed gas (q in mmol g^{-1}) according to the Clausius-Clapeyron equation [43]:

$$\Delta H_{st}=R\frac{d\ln p}{d(1/T)|_{q_e}} \quad (3)$$

where ΔH_{st} (kJ mol^{-1}) is isosteric heat of adsorption, P (bar) is the pressure at a constant equilibrium uptake, T (K) is the temperature and R (J $mol^{-1}K^{-1}$) is the ideal gas constant.

RESULTS AND DISCUSSION

1. Characterization Results

1-1. Chemical Characterization

Table 2 shows the results of ultimate and proximate analysis performed on the broom sorghum stalk and the pristine AC. As a starting material for AC preparation, materials with high volatile organic compounds and carbon content but low in ash content, are desirable. As can be seen from Table 2, broom sorghum stalk has suitable carbon content, high volatile matter and low ash content. As a consequence, it can be an appropriate precursor for the preparation of AC. After carbonization and activation steps the volatile matter content of AC decreased and percent of fixed carbon increased. In addition, the elemental analysis of AC indicates

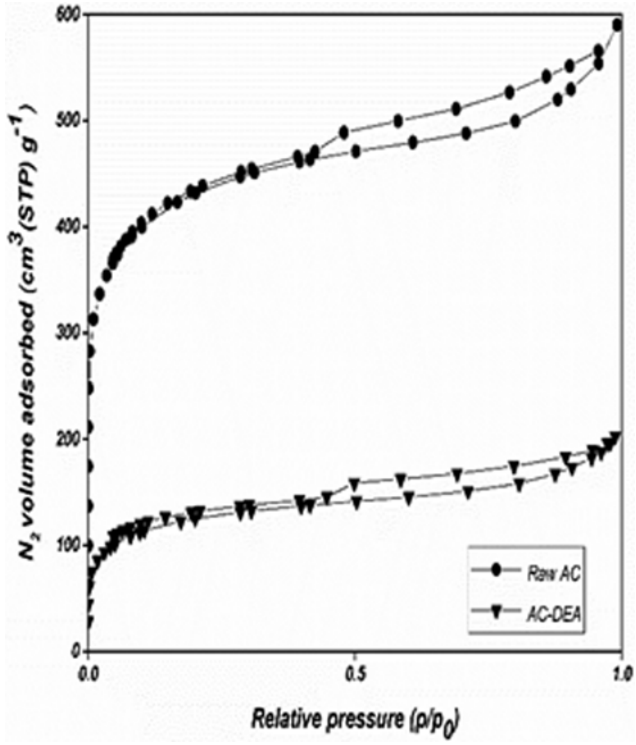

Fig. 2. N_2 adsorption-desorption isotherms of unmodified and modified broom stalks based ACs.

an increase in carbon level and decrease in oxygen content. This is due to the degradation of organic materials and partial decomposition of volatile compounds (mainly cellulose and hemicellulose) under carbonization condition, leaving a high purity carbon.

1-2. Porosity Analysis

Fig. 2 shows the N_2 adsorption-desorption isotherms of the AC before and after amine functionalization. According to the IUPAC classification, these isotherms can be classified as a hybrid between types I and IV with most of the adsorbed volume contained in the micropores. However the presence of mesopores in the structure of the prepared ACs is proved by the hysteresis loop at $P/P_0>0.4$, which resulted in a gradual increase in adsorption after the initial filling of the micropores and a more rapid increase near saturation [44,45]. There were many available empty pores in the structure of the pristine AC which could be used to adsorb the N_2 molecules. Whereas, after amine functionalization some pores had been blocked by the amine creating enormous active sites and there was not enough space for N_2 molecules adsorption. This caused a significant reduction in nitrogen uptake through physisorption.

The size distributions of ACs before and after amine modification derived from (a) a micropore (MP) plot and (b) a Barrett-Joyner-Halenda (BJH) plot are shown in Fig. 3. For both samples, the volume distribution (dVp/drp), especially near to the micropore region, increases, which demonstrates that the prepared ACs have mainly micropores with sizes in the ranges of 0.2-1.2 nm and also have some mesopores.

Table 3 lists the main pore characteristics of unmodified and amine modified ACs, including BET surface area, meso, micro and total pore volume and average pore diameter. Based on the data presented in Table 3, amine functionalization caused a drastic reduction in the surface area and total volume of the pristine AC, which could be explained by blocking behaviors of the amine functional groups. However, the average pore size was increased after amine functionalization. Small pores were filled during functionalization while large pores remained, leading to an increase in the average pore size.

1-3. SEM Analysis

Fig. 4(a) is showing the image of 2 μm pristine AC particle magnified 10,000 times. It is observed from the figure that the structure of the pristine AC has a wide surface porosity with different size, indicating relatively high surface areas. It is estimated that the porous structure of the AC resulted from the evaporation of potassium hydroxide (KOH) during carbonization, leaving the empty space previously occupied by the KOH. Fig. 4(b) shows the image of 2 μm DEA-functionalized AC particle magnified 10,000 times. According to the image, diethanolamine has covered most parts of the surface area and reduced the porous structure of the sorbent. Significant differences were observed between the surface morphologies of the unmodified and DEA-modified ACs, which indicated that DEA was successfully attached into AC structure.

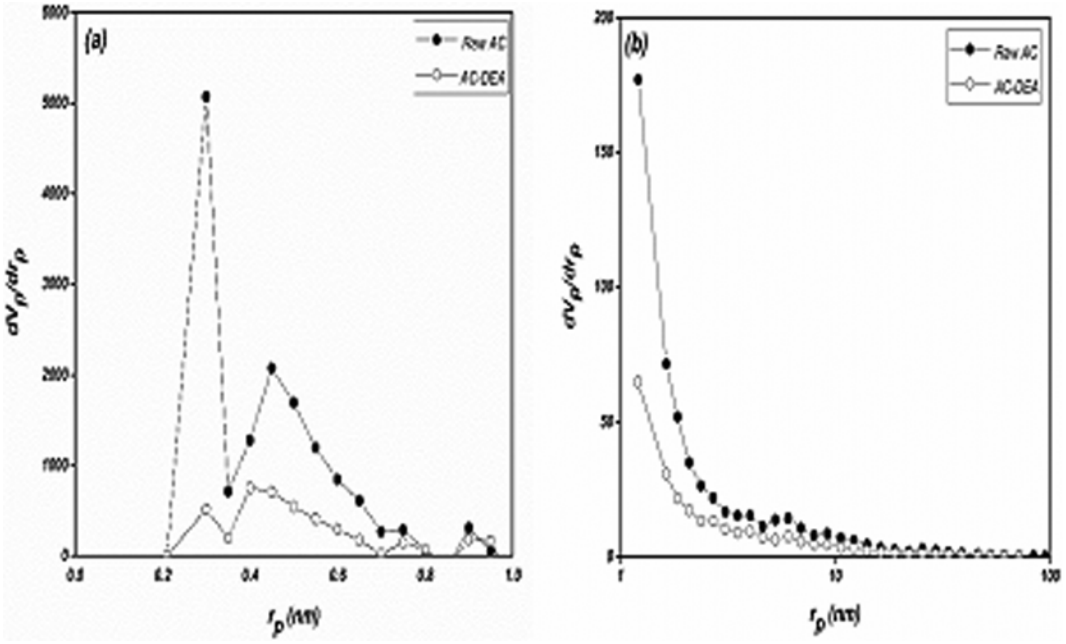

Fig. 3. Micropore (a) and mesopore (b) size distributions of raw AC and functionalized AC obtained by MP and BJH.

Table 3. Textural parameters of the prepared samples

Samples	BET surface area ($m^2\ g^{-1}$)	Micropore volume ($cm^3\ g^{-1}$)	Mesopore volume ($cm^3\ g^{-1}$)	Total pore volume ($cm^3\ g^{-1}$)	Mean pore diameter (nm)
Pristine AC	1619	0.671	0.239	0.910	2.24
AC-DEA	473	0.208	0.105	0.3134	2.64

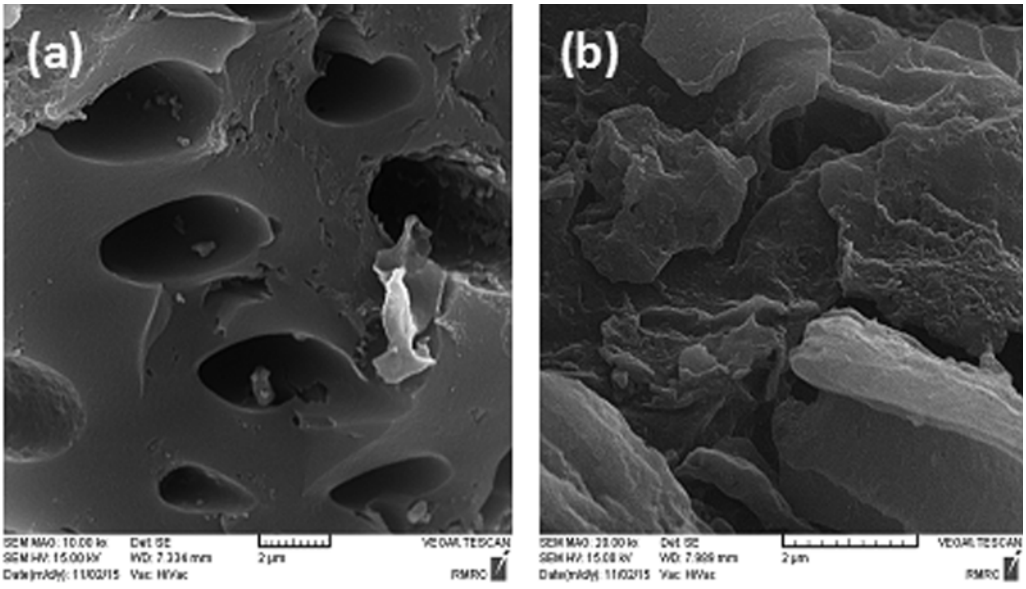

Fig. 4. 2 μm image of (a) unmodified AC and (b) amine-modified AC samples magnified 10,000 times.

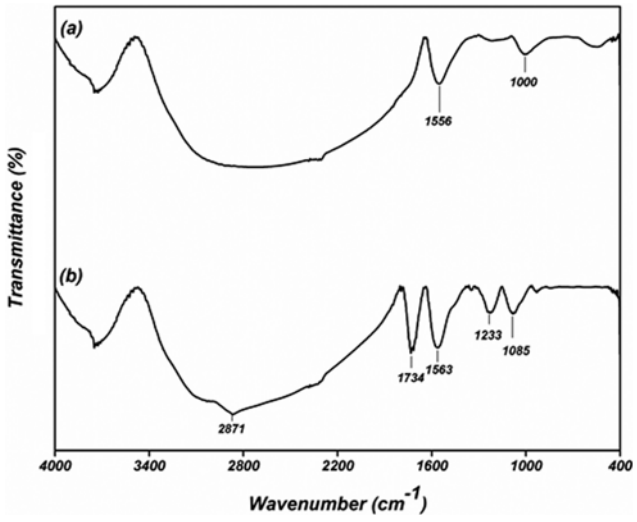

Fig. 5. FTIR spectra of (a) pristine AC and (b) AC-DEA.

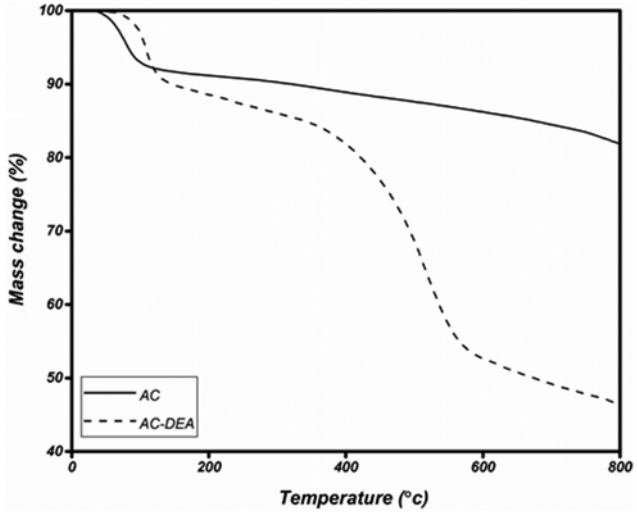

Fig. 6. TGA curves of AC before and after functionalization with DEA.

1-4. FT-IR Analysis

The FT-IR spectra of the unmodified and amine-functionalized ACs are compared in Fig. 5. For both samples the band in the 1,500-1,600 cm^{-1} region is assigned to C=C bond in aromatic rings. In spectrum (a) pertaining to pristine AC, the peak at 1,000 cm^{-1} is assigned to C-O-C stretching vibration. Spectrum (b) is related to the AC functionalized by diethanolamine (AC-DEA). In this spectrum, the peak at 1,734 cm^{-1} denotes the existence of amide (-CO-NH-) groups. The peaks at 2,871 and 1,233 cm^{-1} are assigned to C-N bond stretching. The peak at 1,085 cm^{-1} indicates the C-O stretching vibration in alcohols, ether or ester groups. These observations indicated that DEA was successfully appended into AC structure. Similar analyses were reported in the literature pertaining to the development of carbonaceous adsorbents [46-49].

1-5. TGA Analysis

Thermo-gravimetric analysis (TGA) gives useful information about the functionalized AC because most of the organic functional groups bonded to the adsorbent surfaces are decomposed before the onset of AC weight loss. Fig. 6 shows the TGA analysis curves of the pristine and amine-functionalized AC. TGA curve of the unmodified AC exhibited two main weight loss regions. The first weight loss that occurred below 100 °C was mainly caused by the volatilization of physically adsorbed H_2O, and the second weight loss was due to the decomposition of carbon in the adsorbent structure, whereas, thermal degradation of amine modified AC was a multistage process because of the different functional groups included onto the surface of the adsorbent. For DEA modified sample, the first weight loss region that occurred below 100 °C was attributed to the volatilization of physically adsorbed H_2O similar to unmodified AC. For AC-DEA, the second weight loss peak emerged above 150 °C, corresponding to the decomposition of attached amine

Table 4. Results of the Boehm titrations

AC sample	Carboxyl (meq g^{-1})	Lactone (meq g^{-1})	Phenol (meq g^{-1})	Total acidity (meq g^{-1})	Total basic (meq g^{-1})
AC	0.225	0.175	0.78	1.18	0.81
AC-DEA	0.09	0.28	0.89	1.26	1.607

functional groups. Then, at the final step decomposition of the carbon structure occurred. However, AC-DEA remained stable below 150 °C, which is suitable for the whole adsorption and desorption processes [50-52].

1-6. Boehm Titration Analysis

The acidic and basic functional groups of AC samples were characterized by the classical Boehm method. Table 4 presents the Boehm titration results of AC samples before and after amine functionalization. As expected, nitric acid oxidation introduces a significant number of oxygen containing groups onto the carbon surface. Furthermore, the surface basicity of AC-DEA, which provides chemical adsorption sites for CO_2 molecules bonding, was enhanced as a result of reaction between the carboxyl groups with amine. Additionally, some lactone and phenol groups could react with amino groups forming amide. The AC-DEA had 1.98 times more total surface basic sites compared to the pristine AC [53].

2. Gas Adsorption Results

2-1. Pure Carbon Dioxide and Methane Adsorption Isotherms

Comparison of CO_2 and CH_4 adsorption capacities between pristine AC and AC-DEA samples at different pressures up to 25 bar and three temperatures, 288, 298 and 308 K, is given in Fig. 7. It is clear that the amount of CO_2 and CH_4 adsorption increased by decreasing the temperature and increasing the pressure. Decrease of gas adsorption by increasing the temperature can be related to the fact that adsorption phenomenon on both adsorbents is an exothermic process. Observing Fig. 7, at all temperatures, pristine AC exhibited a higher adsorption capacity of CO_2 over CH_4 but this difference is not significant. The higher adsorption amount of CO_2 can be ascribed to its smaller molecular size, large quadrupole moment and high degrees of polarizability. That is, the interactive forces between CO_2 and pristine AC are bigger than those, the interactive forces, for CH_4. Table 5 shows the quadrupole moment, polarizability and critical diameter of CO_2 and CH_4 [54].

Table 5. Polarizabilities, quadrapole moments and the critical diameters of methane and carbon dioxide

Gas	Polarizability ($\times 10^{25}$ cm^3)	Quadrapole ($\times 10^{40}$ cm^2)	Critical diameter (nm)
CH_4	25.9	0	0.38
CO_2	29.1	−13.71	0.33

After amine functionalization, the AC-DEA sample showed a low adsorption capacity for CH_4 and a high adsorption capacity for CO_2 compared to the raw AC. As expected, the amine functionalization increased the basicity and nitrogen content of the pristine AC. However, it drastically reduced the surface area and the pore volume as previously observed by other authors [27,32,33,55]. Note that the textural properties are the main parameters which influence CH_4 adsorption. After amine modification the surface area and micropore volume decreased from 1,619 to 475 m^2 g^{-1} and 0.671 to 0.208 cm^3 g^{-1}, respectively, due to the pore blockage. The lower CH_4 adsorption capacity of the modified sample compared to the pristine one can be related to the reduction of surface area and micropore volume, which limited its physisorption. In the case

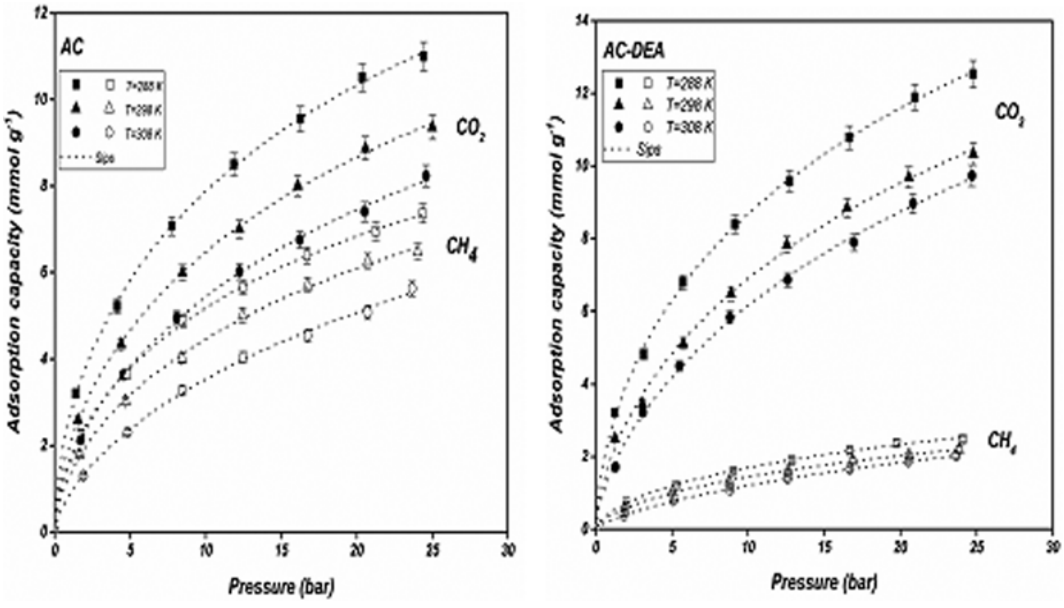

Fig. 7. Pure CO_2 and CH_4 adsorption data and the fitted curves by Sips isotherm model on the pristine AC and AC-DEA at different temperatures.

Table 6. Langmuir, Freundlich and Sips isotherm constants for the adsorption of CO_2 and CH_4 on the unmodified AC

Sample	Equation	Parameters	288 K		298 K		308 K	
			CO_2	CH_4	CO_2	CH_4	CO_2	CH_4
AC	Langmuir	q_{max}	13.577	9.169	12.011	8.751	10.815	8.298
		K_L	0.154	0.143	0.127	0.113	0.109	0.078
		R^2	0.9906	0.9926	0.9918	0.9928	0.9934	0.9950
	Freundlich	K_F	2.926	1.897	2.254	1.477	1.761	0.986
		n	2.372	2.338	2.223	2.115	2.077	1.826
		R^2	0.9983	0.9979	0.9984	0.9980	0.9984	0.9979
	Sips	q_{max}	28.796	18.775	25.938	18.543	24.141	18.001
		K_S	0.0189	0.0166	0.015	0.0138	0.010	0.008
		n	1.729	1.704	1.677	1.611	1.612	1.472
		R^2	0.9996	0.9998	0.9996	0.9991	0.9993	0.9986
AC-DEA	Langmuir	q_{max}	15.927	3.455	14.033	3.136	13.643	2.941
		K_L	0.1295	0.103	0.104	0.091	0.087	0.051
		R^2	0.9864	0.9932	0.9907	0.9944	0.9937	0.9975
	Freundlich	K_F	3.039	0.545	2.183	0.433	1.760	0.279
		n	2.235	2.055	2.032	1.938	1.869	1.591
		R^2	0.9984	0.9980	0.9972	0.9951	0.9982	0.9992
	Sips	q_{max}	37.24	7.780	32.817	7.039	30.537	6.557
		K_S	0.014	0.012	0.0118	0.0102	0.0111	0.009
		n	1.724	1.601	1.610	1.535	1.508	1.343
		R^2	0.9995	0.9988	0.9982	0.9991	0.9987	0.9998

of CO_2 adsorption by AC-DEA, in spite of the decrease in the pores characteristics, the increase in CO_2 adsorption occurred because of the great chemical affinity generated between CO_2 molecules as a Lewis acid and amine functional groups. Therefore, a combination of physical properties and chemical adsorbate-adsorbent interaction may play a role in CO_2 adsorption. As a consequence, the difference in the adsorption capacity between CO_2 and CH_4 was enlarged, which resulted in a high ideal adsorption selectivity for CO_2/CH_4 on amine modified AC.

In this study, equilibrium adsorption data was modeled by means of standard isotherm models: Langmuir, Freundlich and Langmuir-Freundlich (Sips). The values of models parameters were obtained through a nonlinear fit of experimental data at a specific temperature and are shown for both adsorbents in Table 6. The comparison of the correlation coefficient values (R^2) from Table 6 indicates that Sips isotherm model yields a better fit to the experimental data, which demonstrates the heterogeneous nature of the adsorbents' surfaces. With increasing the temperature, the values of K_L, K_F and K_S parameters decreased for both adsorbate, indicating that the affinity between adsorbate and adsorbent had an inverse relationship with temperature, confirming the exothermic nature of the gas adsorption process. These results demonstrated that the adsorption of the CO_2 and CH_4 by unmodified and DEA modified ACs is more favorable at low temperature. The values of Sips exponent, n, for a homogeneous system is equal to one, so higher values of n exhibit that the system is more heterogeneous. According to Table 6, n values decrease with the increase of adsorption temperature, which reveals that at lower temperature the system is more heterogeneous. In addition, at the same conditions, all calculated model parameters of CO_2 are obtained higher than those of CH_4, which shows more tendency of both samples for CO_2 against CH_4. Fitting results using the Langmuir-Freundlich model is also shown for both adsorbents in Fig. 7 along with experimental data.

2-2. Selectivity of CO_2

Considering n_{CO_2} and n_{CH_4} as the amount of CO_2 and CH_4 ad-

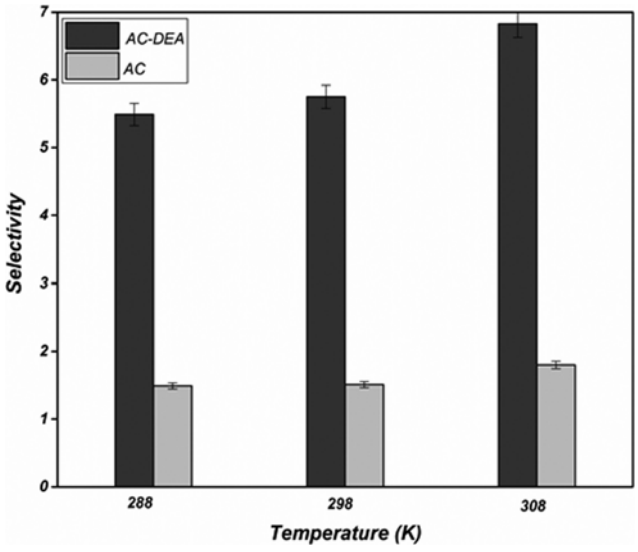

Fig. 8. Idea adsorption selectivity for CO_2/CH_4 system on unmodified and DEA modified ACs.

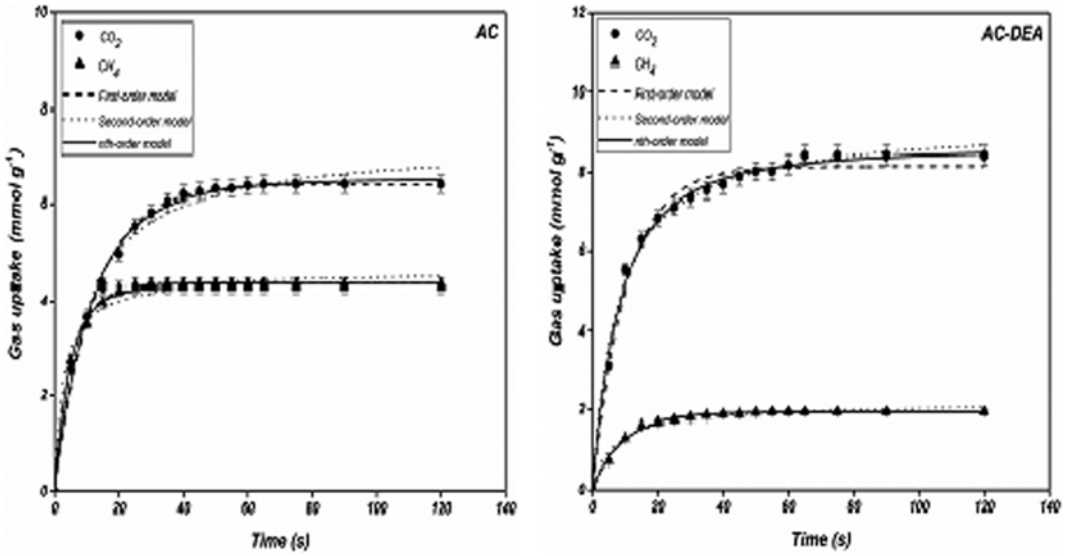

Fig. 9. CO_2 and CH_4 adsorption kinetics of pristine AC and AC-DEA at 298 K and 10 bar.

Table 7. Constants of pseudo-first, second-order and nth-order kinetic models for the adsorption of CO_2 and CH_4 on pristine AC and AC-DEA

Sample	Gas	$q_{e(exp)}$	First-order			Second-order			nth-order			
			q_e	K_1	R^2	q_e	K_2	R^2	q_e	K_n	n	R^2
AC	CO_2	6.51	6.45	0.07	0.998	7.40	0.10	0.989	6.53	0.06	1.12	0.998
	CH_4	4.30	4.29	0.18	0.997	4.63	0.32	0.987	4.31	0.18	1.04	0.998
AC-DEA	CO_2	8.43	8.15	0.09	0.987	9.18	0.13	0.993	8.62	0.03	1.51	0.994
	CH_4	1.94	1.92	0.10	0.995	2.16	0.14	0.978	1.93	0.10	1.03	0.995

sorbed at equilibrium state, Fig. 8 shows the ideal selectivity of CO_2 over CH_4 by unmodified and modified ACs at 1 bar as a function of temperature.

As shown in Fig. 8, the modified AC with a secondary amine (DEA) would lead to a significant improvement in selectivity for CO_2 over CH_4, a requirement for successful application of the sorbents for CO_2 separation. For unmodified AC, the selectivity of CO_2/CH_4 (1.51) is very low, while amine modified AC possess selectivity as high as 5.75 at 298 K and 1 bar. The stronger interaction between amine groups and acidic CO_2 molecules, which is not present in methane, is responsible for the higher selectivity of CO_2/CH_4 on amine-functionalized AC. Furthermore, the temperature increase for both adsorbents resulted in higher selectivity. With respect to CO_2 adsorption properties, increasing temperature has a stronger effect on desorption of CH_4 from the adsorbent surface compared to CO_2, which resulted in higher selectivity of CO_2/CH_4 at higher temperatures. Although, the selectivity of CO_2/CH_4 for AC-DEA is around 6.83 at 308 K.

2-3. Adsorption Kinetics

The kinetics of CO_2 and CH_4 adsorption before and after amine functionalization was investigated at 298 K and 10 bar to obtain an understanding of the adsorption mechanism, including physisorption and chemisorption. The plots of CO_2 and CH_4 adsorption capacity (pure gases experiments) versus time and their corresponding fits to the kinetic models for pristine AC and DEA functionalized AC are shown in Fig. 9.

The data obtained revealed a fast kinetics for the adsorption of CO_2 and CH_4 on prepared ACs in which most of the adsorption occurred at initial period of adsorption experiments and then followed by a slower second stage. This issue is of importance for practical industrial applications because it reduces the cycle time. In all cases the adsorption capacity of the CO_2 molecule is remarkably higher than that of the CH_4 molecule, whereas, the adsorption rate of methane for unmodified and modified samples was faster than that of the CO_2. This is attributed to the fact that strongly adsorbable CO_2 molecule needs more time to achieve a desired amount of adsorption.

Table 7 lists the obtained parameters from the kinetic models, pseudo-first-order, pseudo-second-order and pseudo-nth-order, through a nonlinear fit of experimental data. It was observed that the first-order kinetics provided an adequate description of the physical adsorption of CH_4 on both adsorbents since nth-order model produced a kinetic order close to unity. Furthermore, pseudo-first and pseudo-second order kinetic models presented some limitations with respect to the prediction of CO_2 adsorption on pristine AC and AC-DEA. The adsorption kinetics of CO_2 on both adsorbents was successfully described using nth-order kinetic model with a reaction kinetic order of 1.12 and 1.51, respectively. The value of n recovered by applying nth-order kinetic model indicates that CO_2 uptake onto the AC-DEA may be controlled by a combina-

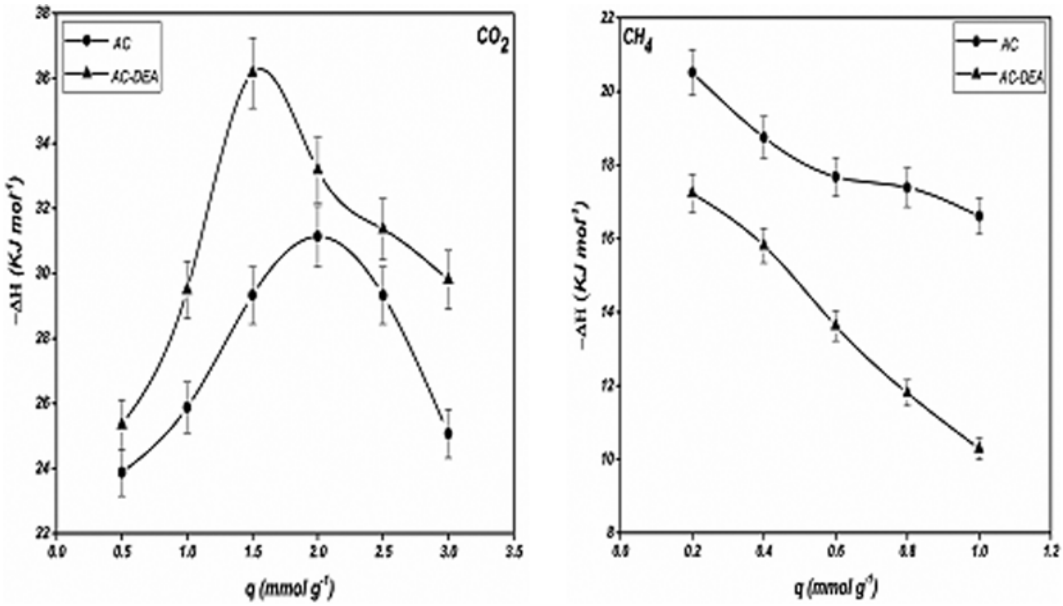

Fig. 10. Isosteric heats of adsorption for methane and carbon dioxide on unmodified and amine modified ACs.

tion of physical and chemical adsorption mechanisms. The value of adjustable parameter, n, for pristine AC indicated that physisorption was the prevailing mechanism in the CO_2 adsorption. After amine modification, a possible change in the mechanism of adsorption from physisorption to predominantly chemisorption happened according to the higher n value compared to pristine AC.

2-4. Adsorption Thermodynamics

In Fig. 10, the isosteric heats of adsorption of CO_2 and CH_4 for pristine AC and AC-DEA are plotted as a function of loading. The negative isosteric heats of adsorption obtained confirmed the exothermic nature of the adsorption processes for both adsorbates. As shown, the isosteric heats of adsorption varied with the surface loading, thereby indicating a heterogeneous adsorption system. For both adsorbents the q_{st} value for CO_2 was higher than that for CH_4, which demonstrates that CO_2 is significantly strongly adsorbed than the CH_4.

With an increase in loading, the isosteric heats for CO_2 exhibit an increasing trend which can be attributed to the adsorbate-adsorbate interactions, followed by a decrease due to active sites filling at the higher surface coverage. This phenomenon can be justified by knowing that strong adsorption sites are occupied first at low coverage due to the high affinity between CO_2 molecules and the adsorbent. Along with the increase of loading, the weaker adsorption sites will be occupied, and the isosteric heats thus decline. For all surface coverage, the amount of heat of adsorption for AC-DEA was higher than pristine AC because of the stronger interaction between CO_2 and AC-DEA adsorbent. The isosteric heat of adsorption of CH_4 decreases as the loading increases. At high surface coverage, a weak interaction between CH_4 and adsorbent occurred due to pore filling, thereby decreasing the heat of adsorption. It is generally accepted that the enthalpy change of physisorption falls within the range 2-21 kJ mol^{-1}, while the chemisorption involves an enthalpy change between 80 and 200 kJ mol^{-1} [53]. From this point of view, both physisorption and chemisorption contribute to the adsorption of CO_2 onto unmodified and amine modified samples, while it is understood that CH_4 is only physically adsorbed onto both sorbents.

3. Comparison of CO_2/CH_4 Adsorption Performance with Other Adsorbents

Table 8 compares the adsorption capacity and equilibrium selectivity for CO_2 and CH_4 on different adsorbents reported in the literature with the adsorbent developed in the present study. For the

Table 8. Comparison of adsorption capacities and equilibrium selectivities for CO_2 and CH_4 on different adsorbents at 1 bar

Adsorbent	P (bar)	T (K)	q_{CO_2} (mmol g^{-1})	q_{CH_4} (mmol g^{-1})	Selectivity (CO_2/CH_4)	Ref.
DEA functionalized AC	1	298	2.13	0.37	5.75	This study
β-Zeolite	1	303	1.29	0.32	4.03	[56]
Hβ-zeolite	1	303	1.35	0.35	3.85	[56]
Palm shell activated carbon	1	298	0.48	0.13	3.56	[15]
PEI-oil palm shell AC	1	298	2.28	0.7	3.26	[15]
Microwave activated carbon	1	298	2.13	0.98	2.17	[8]
MOF-5	1	298	1.91	0.61	3.13	[4]
$Cu_3(BTC)_2$	1	298	2.50	0.91	2.74	[4]

sample of AC-DEA the selectivity of CO_2/CH_4 can reach as high as 5.75, which is much higher than that of other adsorbents shown in Table 8. The high selectivity of CO_2/CH_4 on AC-DEA makes it a promising adsorbent for recovering CH_4 from natural gas and landfill gas.

CONCLUSION

A new type of AC adsorbent was prepared for the adsorptive separation of carbon dioxide and methane. Broom sorghum stalk was utilized as a lignocellulosic solid waste that contains high amounts of carbon for AC preparation. AC was produced from chemical activation of broom stalk by KOH and then was functionalized with diethanolamine (DEA). The effect of activated carbon surface modification through amine functionalization on adsorptive separation of CO_2 and CH_4 was studied from 288-308 K and 0-25 bar. The DEA functionalized AC showed different chemical and textural characteristics with a significant reduction in the surface area and pore volume. In spite of lower porosity, the incorporation of DEA improved the ideal selectivity of CO_2/CH_4 compared to the pristine AC, and the optimum selectivity of CO_2/CH_4 could reach as high as 5.75 at 1 bar and 298 K. Such high adsorption selectivity of CO_2 can be ascribed to chemical adsorbate-adsorbent interaction. The Langmuir-Freundlich isotherm fitted the experimental pure data with the most accuracy for both adsorbates, which indicated the heterogeneous nature of the adsorbents surface. The arbitrary nth-order model was successfully utilized to describe the experimental kinetic data in which the fractional order of reaction was considered as an adjustable parameter. Also, obtained values of isosteric heat of adsorption evaluated by a set of isotherms based on the Clasius-Clapeyron equation indicated the sorption of CO_2 onto the studied ACs is a rather complex process, the mechanism of which may include both physisorption and chemisorption mechanisms, while CH_4 only is physically sorbed on both sorbents. Finally, the results of the present study are promising in terms of improvement in the economy of adsorbent production for applications in natural gas and landfill gas purifications as well as solid waste management.

REFERENCES

1. X. Xu, X. Zhao, L. Sun and X. Liu, *J. Nat. Gas Chem.*, **17**, 391 (2008).
2. M. Mofarahi and F. Gholipour, *Micropor. Mesopor. Mater.*, **200**, 1 (2014).
3. S. S. A. Syed-Hassan and M. S. M. Zaini, *Korean J. Chem. Eng.*, **33**, 2502 (2016).
4. J. Li, J. Yang, L. Li and J. Li, *J. Energy Chem.*, **23**, 453 (2014).
5. M. D. Rad, S. Fatemi and S. M. Mirfendereski, *Chem. Eng. Res. Des.*, **90**, 1687 (2012).
6. Z. Li, G. Xiao, Q. Yang, Y. Xiao and C. Zhong, *Chem. Eng. Sci.*, **120**, 59 (2014).
7. B. C. Bai, S. Cho, H.-R. Yu, K. B. Yi, K.-D. Kim and Y.-S. Lee, *J. Ind. Eng. Chem.*, **19**, 776 (2013).
8. H. Yi, F. Li, P. Ning, X. Tang, J. Peng, Y. Li and H. Deng, *Chem. Eng. J.*, **215**, 635 (2013).
9. J. A. Delgado, M. A. Uguina, J. L. Sotelo, B. Ruíz and M. Rosário, *J. Nat. Gas Chem.*, **16**, 235 (2007).
10. P. Li and F. H. Tezel, *Micropor. Mesopor. Mater.*, **98**, 94 (2007).
11. A. Houshmand, M. S. Shafeeyan, A. Arami-Niya and W. M. A. W. Daud, *J. Taiwan Ins. Chem. Eng.*, **44**, 774 (2013).
12. C. Pevida, M. Plaza, B. Arias, J. Fermoso, F. Rubiera and J. Pis, *Appl. Surf. Sci.*, **254**, 7165 (2008).
13. X. Xu, X. Zhao, L. Sun and X. Liu, *J. Nat. Gas Chem.*, **18**, 167 (2009).
14. M. S. Shafeeyan, W. M. A. W. Daud, A. Shamiri and N. Aghamohammadi, *Chem. Eng. Res. Des.*, **104**, 42 (2015).
15. M. K. Aroua, W. M. A. W. Daud, C. Y. Yin and D. Adinata, *Sep. Purif. Technol.*, **62**, 609 (2008).
16. Y. Li, H. Yi, X. Tang, F. Li and Q. Yuan, *Biochem. Eng. J.*, **229**, 50 (2013).
17. R. Krishna, *Micropor. Mesopor. Mater.*, **156**, 217 (2012).
18. M. S. Shafeeyan, W. M. A. W. Daud, A. Shamiri and N. Aghamohammadi, *Energy Fuels*, **29**, 6565 (2015).
19. A. M. Rashidi, D. Kazemi, N. Izadi, M. Pourkhalil, A. Jorsaraei, E. Ganji and R. Lotfi, *Korean J. Chem. Eng.*, ***33***, 616 (2016).
20. C. Phalakornkule, J. Foungchuen and T. Pitakchon, *J. Sustainable Energy Environ.*, **3**, 153 (2012).
21. W.-J. Liu, F.-X. Zeng, H. Jiang and X.-S. Zhang, *Bioresour. Technol.*, **102**, 8247 (2011).
22. A.-N. A. El-Hendawy, A. J. Alexander, R. J. Andrews and G. Forrest, *J. Anal. Appl. Pyrolysis*, **82**, 272 (2008).
23. M. S. Shafeeyan, W. M. A. W. Daud, A. Houshmand and A. Arami-Niya, *Appl. Surf. Sci.*, **257**, 3936 (2011).
24. D.-I. Jang and S.-J. Park, *Bull. Korean Chem. Soc.*, **32**, 3377 (2011).
25. M. Plaza, C. Pevida, B. Arias, J. Fermoso, A. Arenillas, F. Rubiera and J. Pis, *J. Therm. Anal. Calorim.*, **92**, 601 (2008).
26. M. S. Shafeeyan, A. Houshmand, A. Arami-Niya, H. Razaghizadeh and W. M. A. W. Daud, *Bull. Korean Chem. Soc.*, **36**, 533 (2015).
27. L. Meng, K.-S. Cho and S.-J. Park, *Carbon Lett.*, **10**, 221 (2009).
28. S. Hao, Q. Xiao, H. Yang, Y. Zhong, F. Pepe and W. Zhu, *Micropor. Mesopor. Mater.*, **132**, 552 (2010).
29. A. Sayari, Y. Belmabkhout and R. Serna-Guerrero, *Biochem. Eng. J.*, **171**, 760 (2011).
30. A. Houshmand, W. M. A. W. Daud, M.-G. Lee and M. S. Shafeeyan, *Water Air Soil Poll.*, **223**, 827 (2012).
31. C. Lee, Y. Ong, M. Aroua and W. W. Daud, *Chem. Eng. J.*, **219**, 558 (2013).
32. W. Kangwanwatana, C. Saiwan and P. Tontiwachwuthikul, *Chem. Eng. Trans.*, **35**, 403 (2013).
33. F. Banisheykholeslami, A. A. Ghoreyshi, M. Mohammadi and K. Pirzadeh, *CLEAN-Soil, Air, Water*, **43**, 1084 (2015).
34. X. Feng, N. Dementev, W. Feng, R. Vidic and E. Borguet, *Carbon*, **44**, 1203 (2006).
35. S. Khalili, A. A. Ghoreyshi, M. Jahanshahi and K. Pirzadeh, *CLEAN-Soil, Air, Water*, **41**, 939 (2013).
36. M. Keramati and A. A. Ghoreyshi, *Physica E*, **57**, 161 (2014).
37. M. Delavar, A. A. Ghoreyshi, M. Jahanshahi, S. Khalili and N. Nabian, *RSC Adv.*, **2**, 4490 (2012).
38. S. Khoshhal, A. A. Ghoreyshi, M. Jahanshahi and M. Mohammadi, *RSC Adv.*, **5**, 24758 (2015).
39. K. Foo and B. Hameed, *Chem. Eng. J.*, ***156***, 2 (2010).
40. B. E. Reed and M. R. Matsumoto, *Sep. Sci. Technol.*, ***28***, 2179 (1993).
41. D. Saha, Z. Bao, F. Jia and S. Deng, *Environ. Sci. Technol.*, **44**, 1820

(2010).
42. R. Serna-Guerrero and A. Sayari, *Chem. Eng. J.*, **161**, 182 (2010).
43. S. Himeno, T. Tomita, K. Suzuki and S. Yoshida, *Micropor. Mesopor. Mater.*, **98**, 62 (2007).
44. A. Puziy, O. Poddubnaya, Y. N. Kochkin, N. Vlasenko and M. Tsyba, *Carbon*, **48**, 706 (2010).
45. M. Pérez-Mendoza, C. Schumacher, F. Suárez-García, M. Almazán-Almazán, M. Domingo-García, F. López-Garzón and N. Seaton, *Carbon*, **44**, 638 (2006).
46. J. Figueiredo, M. Pereira, M. Freitas and J. Orfao, *Carbon*, **37**, 1379 (1999).
47. M. S. Shafeeyan, W. M. A. W. Daud, A. Houshmand and A. Shamiri, *J. Anal. Appl. Pyrolysis*, **89**, 143 (2010).
48. F. Avilés, J. Cauich-Rodríguez, L. Moo-Tah, A. May-Pat and R. Vargas-Coronado, *Carbon*, **47**, 2970 (2009).
49. Z. Rozlívková, M. Trchová, M. Exnerová and J. Stejskal, *Synth. Met.*, **161**, 1122 (2011).
50. X. Wang, Q. Guo, J. Zhao and L. Chen, *Int. J. Greenhouse Gas Control*, **37**, 90 (2015).
51. X. Wang, Q. Guo and T. Kong, *Chem. Eng. J.*, **273**, 472 (2015).
52. X. Wang, L. Chen and Q. Guo, *Chem. Eng. J.*, **260**, 573 (2015).
53. G. D. Vuković, A. D. Marinković, M. Čolić, M. Đ. Ristić, R. Aleksić, A. A. Perić-Grujić and P. S. Uskoković, *Chem. Eng. J.*, **157**, 238 (2010).
54. N. Heymans, B. Alban, S. Moreau and G. De Weireld, *Chem. Eng. Sci.*, **66**, 3850 (2011).
55. M. Plaza, C. Pevida, A. Arenillas, F. Rubiera and J. Pis, *Fuel*, **86**, 2204 (2007).
56. X. Xu, X. Zhao, L. Sun and X. Liu, *Chem. Ind. Eng. Prog.*, **12**, 2116 (2009).